International Journal of Chemical and Biochemical Sciences
(ISSN 2226-9614)

Journal Home page: www.iscientific.org/Journal.html

Grated *Agave Americana* – Green corrosion inhibitor for stainless steel in 0.5M H_2SO_4

Rihane BOULMERKA; Sihem ABDERRAHMANE*and Fadila BENACHOUR

Laboratory of Surface Engineering (LIS); Badji Mokhtar – Annaba University, B.P.12 El Hadjar Annaba ALGERIA

Abstract

The Grated *Agave Americana* plant (GAA), from the Algerian Eastern Coast (Annaba) was tested as a corrosion inhibitor of AISI 410 steel in 0.5M H_2SO_4. Stationary electrochemical techniques (Potentiodynamic polarization (PDP)) and transient (Electrochemical Impedance Spectroscopy (EIS) and the method Potential of Zero Charge (PZC)), the weight loss method (WL), scanning electron microscopy associated with X-ray Dispersive Energy Spectroscopy (SEM-EDX) and Atomic Force Microscopy (AFM) were used. The polarization curves reveal that GAA acts as a mixed inhibitor. The steel surface is positively charged. Maximum efficacy is 98.65% to 10% (v/v) after 24 h immersion at 25°C. The inhibitor adsorption on metal surface is physisorbed, and obeys the Freundlich isotherm. The inhibitory efficacy decreases with temperature increase. SEM and AFM micrographs confirm the results obtained by the WL method and the electrochemical methods. GAA is a good corrosion inhibitor of AISI 410 steel in 0.5M H_2SO_4.

Keywords: Corrosion, *Agave Americana*, green inhibitor, AISI 410, 0.5M H_2SO_4

Full length article **Corresponding Author*, e-mail: abderrahmanesihem@yahoo.fr, rayhaneboulmerka@gmail.com and fadila_benachour@yahoo.com

1. Introduction

The corrosion of materials takes place through physico-chemical interactions with their environment, resulting in property modifications of metal often accompanied by functional degradation of this latter (deterioration of its mechanical, electrical properties, etc.). Stainless steel is widely used in industry and in various environments, due to its resistance to degradation by environmental reagents [1, 2].

Stainless steels are currently the widely applied materials in corrosive environments, at different temperatures, but with chloride or other aggressive anions, they are subject to pitting corrosion [3, 4]. AISI 410 belongs to the class of martensitic stainless steels (MSS), which are iron-chromium alloys with Cr>10.5% (by weight) and have resistance and high hardness at a relatively low cost. They are less resistant to corrosion than other types of stainless steels. MSS are generally used as surgical instruments, in the manufacture of cutting tools, valves, aerospace equipment, and the production and refining of petroleum etc. [5-8].

Among the methods of protecting metals from corrosion, the use of inhibitors is the simplest and most economical. Therefore, many organic compounds were used as corrosion inhibitors of various metals in different media. Generally, heterocyclic organic compounds containing N, O, and S in aromatic or long chain carbon were reported as effective inhibitors [9–12]. Since these inhibitors are expensive, toxic and have harmful effect on the environment, these properties restrict their use as inhibitors of metals and alloys in various media [13–15]. Hence the orientation of research towards plant extracts because of their profitability, their abundant availability and their environmental acceptability. The presence of alkaloids, flavonoids, tannins, cellulose and polycyclic compounds in plant extracts, facilitates the film formation on the metallic surface preventing corrosion [16]. Thus, plant extracts exhibit good inhibiting activity from corrosion.

This work is focused on understanding the corrosion phenomenon of martensitic stainless steel AISI 410 in 0.5M sulfuric acid solution, either with or without Grated *Agave Americana* (GAA) as a green inhibitor. The GAA inhibitory effect on corrosion of steels in different acidic media was studied [17-20]. Several works were published, using different parts of plants and their extracts as green inhibitors of steels corrosion in different acidic media. Among which the extract of *Opuntia Ficus Indica* [21-23], the extract of leaves of *Cistus ladanifer* [24], the extract of Aloe Vera [25,26], henna [27], *Oxandra asbecki* [28], *Argemone mexicana* [29], *Azadirachta indica* [30], *Mentha pulegium* [31], Damsissa [32], *Ananas comosus* [33], *Lasianthera*

africana [34], *Carica papaya* [35], *Justicia gendarussa* [36], fruit peels [37], *Ferula gummosa* [38], *Ephedra sarcocarpa* [39], *Calligonum comosum* [40], *Salvia officinalis* [41], *Armoracia rusticana* [42], *Myristica fragrans* [43], *Cuscuta reflexa* [44], *Sida cordifolia* extract [45], Dardagan fruit extract [46], *Mimusaps Elangi* extract [47], and *Macaranga Peltata* leaf extract [48].

The study of corrosion was carried out by the weight loss method, Electrochemical Impedance Spectroscopy (EIS), Potentiodynamic Polarization (PDP), and Potential of Zero Charge (PZC), as well as characterization techniques of the surface and adsorbed film such as Scanning Electron Microscopy associated with X-ray Dispersive Energy Spectroscopy (SEM-EDX), Atomic Force Microscopy (AFM) and Fourier-Transform Infrared spectroscopy (FT-IR).

2. Materials and methods

The material used in this study is a martensitic stainless steel (AISI 410) coming from WITTEX brand orthodontic pliers, with the following chemical composition: 0.15% C, 13.04% Cr, 0.18% Mn, 0.39% Si, 0.029% P, 0.020% S, 0.130% Cu, 0.008% Al, 0.003% Ti, 0.024% Nb, 0.269% Ni, 0.040% Mo, 0.031% V, 0.009% Sn, Fe (balance), was obtained by the Atomic Emission Spectroscopy technique (AES). We used a sulfuric acid solution (H_2SO_4) at 0.5 M, obtained from the concentrated acid at 98% brand Biochem, and volume 100ml.

We used the GAA (figure 2) as a green corrosion inhibitor, the latter coming from the Algerian eastern coast (Annaba), it was washed with distilled water and then peeled to remove the hard green layer, finally grated in order to collect a green liquid which we used directly in our experiments.

2.1. Weight loss method

The weight loss measurements are made at different immersion times (2, 4, 6, 8, 10, 12, 14, 16, 18, 20, 22, and 24h), all at an ambient temperature of 25°C. The orthodontic pliers were cut into semi-cylindrical shaped pieces with a surface area of 4.28 cm^2. The sample was then polished, washed with distilled water and acetone, air-dried and weighed before being immersed in different solutions, namely: 0.5 M H_2SO_4 and 0.5M H_2SO_4 at various concentrations (1.5:5; and 10%) (v/v) of GAA, in order to calculate the corrosion rate (Vc) according to equation (1) below, and the inhibitory efficacy (I.E %) using equation (2).

$$V = \frac{\Delta m}{S.t}, \qquad (E1)$$

Where, Δm: mass variation (g); S: metal surface (mm^2); t: time (h).

$$IE\ \% = \frac{Vc - Vc\,inh}{Vc}.100, \qquad (E2)$$

Where, Vc_{inh} and Vc represent the corrosion rates either with and without inhibitor, respectively.

2.2. Electrochemical methods

The study of AISI 410 stainless steel electrochemical behavior in 0.5M H_2SO_4 either with or without use of GAA was first carried out using the Electrochemical Impedance Spectroscopy (EIS) method, proceeding by a scan from high frequencies 10 kHz (HF) to low frequencies 10 mHz (LF) with a sinusoidal disturbance of 10 mV per decade.

Semi-circular curves were obtained for stainless steel AISI 410 in 0.5M H_2SO_4 either with or without use of inhibitors at different concentrations. From EIS spectra fit, all of the charge transfer resistance (R_{ct}), the solution resistance (Rs) and the double layer capacitance (C_{dl}) were obtained.

The inhibitory efficacy was calculated according to equation (3).

$$IE(\%) = \left(\frac{R_{ct} - R_{ct}^{\circ}}{R_{ct}}\right) \times 100, \qquad (E3)$$

Where, R_{ct} and R_{ct} are the charge transfer resistances with and without use of inhibitor, respectively. The polarization resistance (Rp) can be calculated using equation (4) below.

$$Rp = \frac{R_L \times R_{ct}}{R_L + R_{ct}}, \qquad (E4)$$

In a second time, by the potentiodynamic polarization method with a scan potential from -800 mV to 0 mV/(Ag/AgCl) with 1mV/s scan rate. The inhibitor efficacy is calculated according to equation (5).

$$IE(\%) = \left(\frac{i_{corr}^{\circ} - i_{corr}}{i_{corr}^{\circ}}\right) \times 100, \qquad (E5)$$

Where, i°_{corr} and i_{corr} are the respective values of steel corrosion current without and with inhibitor.

The aim of potentiodynamic curves is to determine the polarization resistance and the corrosion rate. The Tafel plots allow us to reach directly the current density values, as can be deduced from the Stern and Geary equation (6):

$$i_{corr} = \frac{1}{2.3\,Rp}\frac{(\beta a.\beta c)}{(\beta a + \beta c)}, \qquad (E6)$$

It is to be noted that all electrochemical tests are carried out using a Gamry interface 1000 Potentiostat/Galvanostat managed with the Gamry Framework software. The whole system is connected to an electrochemical glass cell and a thermostatic double wall with three electrodes: a stainless steel AISI 410 working electrode coated in a 0.6 cm^2 epoxy resin, a reference electrode (Ag/AgCl), and a plate platinum auxiliary electrode, bearing an immersion time of 2 hours.

Before each electrochemical test, the working electrode undergoes a polishing using abrasive paper with different grain sizes (SiC: 800, 1200, 2400 and 4000), followed by a distilled water rinse, and a degreasing with

methanol before drying with cold air. A sulphuric acid solution (H_2SO_4) at 0.5 M was used for electrolyte.

2.3. Surface analyses

FT-IR spectroscopy was applied to GAA to identify functional groups. The spectra were recorded on the KBr powder (PERKIN ELMER Spectrum RX/FT-IR System).

The morphology and composition of the inhibitive films on surface after 2 h immersion of AISI 410 stainless steel in 0.5M H_2SO_4, either with or without inhibitor were examined by SEM-EDX, and AFM.

3. Results and discussion

3.1. Weight loss method and surface morphology

Table 1 gathers the results, obtained by the gravimetric method, of AISI 410 behavior to corrosion in 0.5M H_2SO_4 at 25°C, without and with GAA at different concentrations (1.5: 5 and 10 % (v/v)). The AISI 410 corrosion rate without GAA after 24 hours is 156,410 $\mu g.mm^{-2}.h^{-1}$, while with 1.5% (v/v) GAA, it dropped to 5.248 $\mu g.mm^{-2}.h^{-1}$ corresponding to 96.64% maximum efficacy. The presence of 5% (v/v) GAA, gives a corrosion rate 3.843 $\mu g.mm^{-2}.h^{-1}$ with 97.54% efficacy. By doubling this last concentration, the rate is 2.106 $\mu g.mm^{-2}.h^{-1}$and the efficacy improved (98.65%).

The inhibitory efficacy variation of GAA on AISI 410 corrosion in 0.5 M H_2SO_4 according to time is represented in figure 3. We observe that the concentration increase raises the inhibitor efficacy, and for each study concentration, corresponds a maximum efficacy after 24h immersion; for the concentration 1.5% (v/v) GAA the efficacy is 96.64%, for 5% (v/v) GAA, the efficacy is 97.54% and for 10% (v/v) GAA, the efficacy is 98.65%.

The surface morphologies of AISI 410 immersed during 2 h in 0.5 M H_2SO_4 either with or without 10% (v/v) GAA, were investigated by SEM. The AISI 410 micrographs analysis, without inhibitor (figure 12), present a very rough surface with the apparition of pitting corrosion, which can be attributed to sulfuric acid attack. However, with inhibitor, the AISI 410 surface (figure 14) is smooth with an inhibitor film formation covering the entire surface. SEM observations confirmed the gravimetric results.

3.2. Electrochemical methods

3.2.1. Open circuit potential (OCP)

Figure 4 shows the open circuit corrosion potential (OCP) according to time of AISI 410 in 0.5M H_2SO_4 either with or without 10% (v/v) GAA, after 2 hours immersion at 25°C. We note that without inhibitor, the corrosion potential (E_{corr}) stabilizes after 5800s with a -0.490V/Ag/AgCl value. The addition of 10% (v/v) GAA shifts the potential towards positive values till -0.445V/Ag/AgCl, while with GAA, causes a displacement of E_{corr} towards more noble values compared to those without, indicating a protective film presence adsorbed on the steel surface.

3.2.2. Electrochemical impedance spectroscopy (EIS)

The electrochemical impedance diagrams relate the adsorption behavior of the inhibitory molecules on the steel surface, in representation of Nyquist (figure 5.a). We note from these spectra at different inhibitor concentrations (0; 1.5; 2; 5; 7 and 10% (v/v)), the presence of two loops, the first capacitive, whose diameter raises with the inhibitor concentration increase, which is due to the charge transfer phenomenon, followed by a second inductive loop due to the relaxation of the adsorbed species at metal-solution interface. The adsorption of organic molecules increases the charge transfer resistance and decreases the double layer capacity at metal-electrolyte interface, which is due to the reduction of the dielectric constant between metal and electrolyte.

From Bode representation according to the phase angle (figure 5.b), we observe the presence of a single time constant linked to capacitive semicircles, indicating that the corrosion phenomenon is mainly controlled by charge transfer [49]. For the representation of Bode according to the module (figure 5.c), we note that the concentration increase of GAA favors the polarization resistance increase.

The results of electrochemical impedance spectroscopy were well adjusted with the equivalent electrical circuit $R_1+Q_1/(R_2+L_1/R_3)$.

The simulated equivalent electrical circuit (figure 5.d) consists of an electrolyte resistance ($R_s = R_1$) in series with a constant phase element ($CPE_{dl} = Q_1$) in parallel with a charge transfer resistance ($R_{ct} = R_2$) and an induction ($L = L_1$) and this latter in parallel with an induction resistance ($R_L = R_3$).

From the electrochemical parameters deduced from the AISI 410 Nyquists in 0.5M H_2SO_4 with GAA at different concentrations, after 2 h immersion (Table 2), we observe that the concentration increase of GAA induces firstly, the decrease in the double layer capacity $(CPE)_{dl}$ at metal-electrolyte interface, from (845 to 162) 10^{-6} $\mu F.cm^{-2}$, and secondly, the increase of charge transfer resistance (R_{ct}) from 12.32 to 116 $\Omega.cm^{-2}$, as well as an increase of the inhibitor efficacy (IE%) upto 89.38% at 10% (v/v) GAA, these variations might be due to the dielectric constant reduction between metal and electrolyte, to the adsorption of the GAA organic molecules and to thickness increase of the protective film.

3.2.3. Potentiodynamic polarization

Figure 6 represents the potentiodynamic polarization curves (Tafel) of AISI 410 in 0.5M H_2SO_4 ,with or without GAA at different concentrations, after 2 h immersion, at 25°C. The shape of the Tafel lines provides information on the steel surface activity, the corresponding

charge transfer reactions as well as the reaction mechanism deduced from the anodic and cathodic slopes [50].

We find that the concentration increase of GAA decreases the densities of anodic and cathodic currents and shifts the corrosion potential towards ennobling compared to those without inhibitor. If the variation in the corrosion potential ΔE_{corr} > 85 mV compared to that without, the inhibitor is considered to be anodic or cathodic. Whereas, if ΔE_{corr} < 85 mV, it is of mixed type [51, 52]. This leads us to conclude that GAA is a mixed type corrosion inhibitor. It affects anodic reactions during the metal dissolution and cathodic reactions during the hydrogen release.

According to the electrochemical parameters deduced from the AISI 410 polarization curves in 0.5M H_2SO_4without and with GAA at different concentrations, after 2h immersion (Table 3). We note that the concentration increase of GAA induces the reduction of the corrosion current density from 1120.27 to 69.160 µA.cm^{-2} and the corrosion potential increase from -467.614 to -440.085 mV/Ag/AgCl, of the polarization resistance from 0.02 to 1.606 Ω.cm^{-2}, and the inhibitor efficacy upto 93.83% corresponding to 10^{-4}M. GAA is a good corrosion inhibitor of AISI 410, in 0.5 M H_2SO_4.

According to the comparative curves of AISI 410 inhibitor efficacies in 0.5M H_2SO_4 in terms of GAA concentrations (figure 7), we observe that the concentration increase raises the inhibitor efficacy. Thus the best efficacy obtained by each method, namely (WL, EIS and PDP) is 59.96; 89.38 and 93.83% respectively, corresponding to the concentration of 10% (v/v) GAA.

3.3. Method of potential of zero charge (PZC)

The adsorption of GAA molecules was studied by the potential of zero charge method. The obtained curve represents a parabola whose peak corresponds to the potential at zero charge E_{PZC}=-0.500V/Ag/AgCl (figure 8). The rational corrosion potential of Antropov (Er) is calculated according to the following equation (7):

$$E_r = E_{ocp} - E_{PZC} \qquad (E7)$$

The value of Er=+0.05V, which allows us to conclude that steel surface is positively charged; indicating that anion adsorption is favored.

3.4. Adsorption isotherms

To understand the interactions between GAA molecules on AISI 410 steel surface, we plotted the following adsorption isotherms: Langmuir, Temkin, Freundlich, Frumkin, Flory-Huggins and El-Awady et al., according to their respective equations (8), (9), (10), (11), (12) and (13):

$$\text{Langmuir} \quad \frac{C_{inh}}{\Theta} = \frac{1}{K_{ads}} + C\_inh \qquad (E8)$$

$$\text{Temkin} \quad e^{-2a\Theta} = K_{ads}C_{inh} \qquad (E9)$$

Freundlich

$$\log\Theta = \log K_{ads} + n\log C \qquad (E10)$$

Frumkin

$$\frac{\Theta}{1-\Theta}e^{(-2a\Theta)} = K_{ads}C_{inh} \qquad (E11)$$

Flory − Huggins

$$\log\frac{\Theta}{C} = \log K_{ads} + a\log(1-\Theta) \qquad (E12)$$

El − Awady *et al.*

$$\log\left(\frac{\Theta}{1-\Theta}\right) = \log K_{ads} + y\log C \qquad (E13)$$

Where: K_{ads} is the equilibrium constant of the adsorption process; Θ is the recovery rate of metal surface. The recovery rates of metal surface (θ) were calculated from the electrochemical impedances, at different concentrations of GAA, and it is calculated according to the equation (14).

$$\theta = \frac{IE(\%)}{100} \qquad (E14)$$

From table 4, the slope values and the regression coefficient (R^2) for the isotherms of Langmuir, Temkin, Freundlich, Frumkin, Flory-Huggins and El-Awady et al., are respectively (1.005,0.988); (0.165,0.971); (0.229,0.994); (0.814,0.917); (-0.994,0.788); (0.885,0.916). The GAA adsorption in 0.5M H_2SO_4 obeys to Freundlich isotherm (figure 9) whose regression coefficient is very close to unity, and the slope values were used to calculate the standard free energy of adsorption (ΔG^o_{ads}).

The adsorption equilibrium constant (K_{ads}) is linked to the standard free energy of adsorption (ΔG^o_{ads}) by Gibbs equation (15):

$$\Delta G^0_{ads} = -RT\ln(1000\ K_{ads}) \qquad (E15)$$

Where, R:perfect gases constant (R= 0,008314 kJ.mol^{-1}.K^{-1}); T: temperature (K); The value 1000 is water concentration in the solution in (g.L^{-1}).

According to R. Idouhli *et al.* [53], if the ΔG^o_{ads} value is between -20 and - 40 kJ.mol^{-1}; both physisorption and chemisorption contribute to the inhibitor adsorption on metal surface. In addition, the negative sign indicates that the adsorption is spontaneous. Generally, if $\Delta G^o_{ads} \leq$ -20 kJ.mol^{-1}, it is a physisorption associated with an electrostatic interaction between charged inhibitor molecules and metal surface; and if $\Delta G^o_{ads} \geq$- 40 kJ.mol^{-1}, then it is a chemisorption based on charge sharing or transfer of inhibitor molecules at metal surface to form coordination bonds [54].

In our study, ΔG^o_{ads}=-15.487kJ.mol^{-1}. Indicating that the adsorption is spontaneous [55, 56] and of physisorbed type [57].

3.5. Surface analyses

According to the micrographs (SEM) of AISI 410 surface (figures 10.a and 10.b), we observe a smooth and homogeneous surface. The AFM micrograph of AISI 410 (figure 11), confirms the observations made by SEM, with a

roughness (Ra) of 83.450 nm. From figures 12.a and 12.b, we observe that AISI 410 surface, immersed in 0.5M sulfuric acid for 2 hours, is corroded under the form of pitting with different sizes; which means that we are in presence of pitting corrosion. The AFM micrograph of AISI 410 (figure 13) confirms the pitting presence under the form of dark areas, distributed on the surface, whose reliefs constitute corrosion products, with 109.863 nm roughness.

According to SEM micrographs (figures 14.a and 14.b), of the surface of AISI 410 in 0.5M H_2SO_4, with 10% (v/v) GAA, we note that the pitting number decreased; which is due to the inhibitor film presence. The AFM micrograph of AISI 410 in 0.5M $H_2SO_4$with 10% (v/v) GAA (figure 15), confirms a significant reduction in pitting number by the adsorption of inhibitory molecules on steel surface, forming an inhibitory film, hence inducing a decrease in roughness (Ra= 29.154 nm). Figure 16 represents the EDX spectra of AISI 410 after 2h immersion, in 0.5M H_2SO_4 either with or without 10% (v/v) GAA. Mass percentages, of different formed elements, are gathered in table 5. In comparison with the composition of AISI 410 either with or without 10% (v/v) of GAA, there is a diminution in the O and Cu contents. The increase in Cr and Fe content, confirms the protective film formation of AISI 410 in the case of inhibited solution. C content increases as well, which is mainly linked to organic molecules adsorption of the inhibitor on the AISI 410 surface.

3.5.1. Temperature effect

In order to determine the thermodynamic parameters, we studied the temperature effect, by plotting the potentiodynamic polarization curves of AISI410 in 0.5M H_2SO_4, either with or without 10% (v/v) GAA, after 2h immersion at temperatures 25, 35 and 45°C. Figure 17 represents the temperature effect on the polarization curves of the AISI 410 in 0.5M H_2SO_4 either with or without 10% (v/v) GAA, after 2h immersion. According to which, we observe the decrease in the current density of the cathode and anode branches, at temperatures 25 and 45ºC, compared to those without as well as the displacement of the corrosion potential towards ennobling. While at 35ºC, we notice a slight diminution in the current density of the anode branch only compared to that without. Which leads us to conclude that GAA acts better at room temperature (25°C) and this was confirmed by its inhibitor efficacy value (93.83%) and its polarization resistance that increased (table 6).

Thermodynamic parameters (activation energy E_a, Enthalpy $\Delta H_a°$, Entropy $\Delta S_a°$) could be determined using the two Arrhenius expressions. The first representation of Arrhenius equations (16) allows calculating the activation energy (E_a) at various temperatures. Figure 18 shows the straight line, log i_{corr} = f(1/T), of AISI 410 stainless steel in 0.5M H_2SO_4either with or without 10% (v/v) GAA:

$$\log_{i_{corr}} = -\frac{E_a}{2.303RT} + \log A \qquad (E16)$$

Where, i_{corr}: corrosion current density (µA.cm^{-2}); A: Arrhenius constant; E_a: activation energy (kJ.mol^{-1}); R: perfect gases constant (J.mol^{-1}.K^{-1}) and T: Absolute temperature (K). The second representation of Arrhenius equation (17) determines both the variation of the standard activation enthalpy ($\Delta H°_a$) and the variation of the standard activation entropy ($\Delta S°_a$). Figure 19 shows the straight line ln (i_{corr}/T) according to (1/T), of AISI 410 in 0.5M H_2SO_4either with or without 10% (v/v) GAA. The $\Delta H°_a$ and $\Delta S°_a$ values are calculated with ($-\Delta H°_a/R$) slope and an interception of (ln $(R/Nh)+\Delta S°_a/R$), respectively.

$$\ln(i_{corr}/T) = \ln(R/Nh) + (\Delta S_a^0/R) - \Delta H_a^0/RT \qquad (E17)$$

Where, h: Planck constant (6.626.10^{-34} J.s); N: Avogadro number (6.022×10^{23}); $\Delta H°_a$: variation of standard activation enthalpy and $\Delta S°_a$: variation of standard activation entropy.

From Table 7, we observe that the value of the activation energy calculated in the presence of 10% (v/v) GAA is lower than that in the absence of inhibitor. The value of the activation energy (Ea) is known to be essential in order to determine the type of the adsorption process (physisorption or chemisorption) for the corrosion reaction of metal in different corrosive media. An explanation of the fact that Ea in the presence of GAA is smaller than that in H_2SO_4, according to Rodovici, cited by Popova *et al*. [58], lower down Ea values in solutions containing inhibitor indicate a specific type of adsorption of the inhibitors, the adsorbed inhibitor's molecules block an essential part of the active sites on the metal surface which is energetically inhomogeneous. In general the adsorbed species block the most active sites, i.e. those with the lowest Ea value. This result was consistent with results from previous studies [59, 60]. The $\Delta H_a^\circ < 0$ valuesindicate that steel dissolution is exothermic [61]. The $\Delta S_a°$ negative values with GAA denote a decrease in molecular disorder provoked by the formation of a complex of adsorbed metal/species. This implies a diminution in steel dissolution inducing an increase of inhibitor efficacy [62].

3.6. FT-IR spectroscopy

Figure 20 shows the FT-IR spectrum of the GAA inhibitor film, formed on AISI 410 surface after 2h immersion in 0.5 M H_2SO_4. The peak that appears at 3462.06 cm^{-1} is attributed to OH stretching band. The peak at 1637.81 cm^{-1} is the result of stretching C = O, which is lower than that of normal C = O, due to resonance. In general, conjugation weakens the absorption. The peak at 667.29 cm^{-1} corresponds to the N-H stretching. The main characteristics of corrosion inhibitors are the presence of oxygen and nitrogen in GAA. Furthermore, several studies showed that the presence of hydroxyl and carbon double bond in an organic compound confirms its inhibiting effect of corrosion [63-66].

Table 1. Corrosion rates of AISI 410 steel in 0.5M H_2SO_4, either with or without GAA at various concentrations and calculated inhibitory efficacies

	0.5M H_2SO_4	1.5% (v/v) GAA		5% (v/v) GAA		10% (v/v) GAA	
Immersion time (h)	V ($\mu g.mm^{-2}.h^{-1}$)	V ($\mu g.mm^{-2}.h^{-1}$)	IE (%)	V ($\mu g.mm^{-2}.h^{-1}$)	IE (%)	V ($\mu g.mm^{-2}.h^{-1}$)	IE (%)
0	/	/	/	/	/	/	/
2	10.182	8.884	12.75	7.589	25.46	4.077	59.96
4	21.193	12.090	42.95	9.083	57.14	7.008	66.93
6	26.915	10.969	59.24	9.730	63.85	5.320	80.23
8	34.601	13.494	61.00	12.523	63.80	8.006	76.86
10	48.069	18.230	62.06	17.103	64.42	11.193	76.71
12	64.269	20.518	68.07	15.160	76.41	15.193	76.36
14	73.524	14.132	80.78	10.642	85.52	8.082	89.00
16	87.420	13.194	84.91	10.246	88.28	9.080	89.61
18	110.963	14.111	87.28	10.794	90.27	8.753	92.11
20	125.630	12.973	89.67	9.889	92.13	7.161	94.30
22	135.462	11.688	91.37	9.627	92.89	9.143	93.25
24	156.410	5.248	96.64	3.843	97.54	2.106	98.65

Table 2. Electrochemical parameters deduced from the AISI 410 Nyquists in 0.5M H_2SO_4 with GAA at different concentrations, after 2h immersion at 25°C and calculated inhibitory efficacies

Parameters / [GAA] % (v/v)	R_s ($\Omega.cm^{-2}$)	R_{tc} ($\Omega.cm^{-2}$)	CPE_{dl} ($\mu F.cm^{-2}$)	*n*	*L* (*H*)	R_L ($\Omega.cm^{-2}$)	R_p ($\Omega.\ cm^{-2}$)	*IE* (%)
0	2.53	12.32	0.000845	0.946	1.790	1.012	0.935	/
1.5	2.97	28.74	0.000392	0.949	1.956	3.642	3.232	57.13
2	2.32	30.00	0.000350	0.927	0.953	3.131	2.835	58.93
5	2.42	47.24	0.000291	0.880	1.523	5.028	4.544	73.92
7	2.22	58.8	0.000178	0.900	1.00	5.394	4.941	79.05
10	2.77	116	0.000162	0.918	0.783	3.243	3.155	89.38

Table 3. Electrochemical parameters deduced from the AISI 410 polarization curves in 0.5M H_2SO_4 either with or without GAA at different concentrations and calculated inhibitor efficacies

Parameters / *[GAA] % (v/v)*	*$-E_{corr}$ ($mV/_{Ag/AgCl}$)*	*i_{corr} ($\mu A.cm^{-2}$)*	*β_a ($mV.dec^{-1}$)*	*β_c ($mV.dec^{-1}$)*	*Rp ($\Omega.cm^{-2}$)*	*IE (%)*
0	467.614	1120.270	57.5	136.7	0.020	-
1.5	451.755	241.222	30.0	119.9	0.043	78.47
2	448.600	230.900	32.6	120.9	0.048	79.39
5	446.747	159.876	31.2	131.1	0.068	85.73
7	444.890	75.450	29.8	114.5	0.182	93.26
10	440.085	69.160	32.9	115.1	1.606	93.83

Table 4. Adsorption isotherms of AISI 410 in 0.5M H_2SO_4 with GAA

Adsorption Isotherm	R^2	Slope
Langmuir	0.988	1.005
Temkin	0.971	0.165
Freundlich	0.994	0.229
Frumkin	0.917	0.814
Flory- Huggins	0.788	-0.994
El-Awady *et al.*	0.885	0.916

Table 5. EDX analysis (% by weight) of the surface composition of AISI 410 before and after immersion in 0.5M H_2SO_4 without and with 10% GAA

Elements (% weight)	C	O	Cu	Si	S	Ca	Cr	Fe
AISI 410	2.52	-	-	0.32	-	0.06	12.07	85.05
AISI410 +0.5M H_2SO_4	2.09	13.37	3.96	0.35	2.84	0.14	10.35	66.89
AISI 410 +0.5M H_2SO_4+ 10%(v/v) GAA	5.19	3.02	2.99	-	-	-	11.23	77.57

Table 6. Electrochemical parameters deduced from the polarization curves of AISI 410 in 0.5M H_2SO_4 either with or without 10% (v/v) GAA at different temperatures and calculated inhibitor efficacy, after 2h immersion

T (°C) / *Parameters*	*25*		*35*		*45*	
	0.5M H_2SO_4	*0.5M H_2SO_4 + 10%(v/v) GAA*	*0.5M H_2SO_4*	*0.5M H_2SO_4 + 10%(v/v) GAA*	*0.5M H_2SO_4*	*0.5M H_2SO_4 + 10%(v/v) GAA*
$-E_{corr}$ ($mV/_{Ag/AgCl}$)	467.614	440.085	472.951	417.327	469.347	427.137
i_{corr} ($\mu A.cm^{-2}$)	1120.270	69.160	1516.778	884.438	1536.002	786.927
β_a ($mV.dec^{-1}$)	57.5	32.9	68.6	35.7	41.3	26.6
β_c ($mV.dec^{-1}$)	139.9	115.1	90.9	144.0	33.5	82.2
Rp ($m\Omega.cm^{-2}$)	136.70	160.64	150	100	60	45
IE (%)	-	93.83	-	41.69	-	48.77

Table 7. Thermodynamic parameters and activation energy of AISI 410 in 0.5M H_2SO_4 10% (v/v) GAA

Solutions / Parameters	0.5M H_2SO_4	0.5M H_2SO_4 +10%(v/v) GAA
E_a (kJ.mol^{-1})	101.011	97.885
ΔH_a°(kJ.mol^{-1})	98.346	-152,074
ΔS_a°(J.mol^{-1}.K^{-1})	143.882	-673.465

Fig.1. Orthodontic Pliers

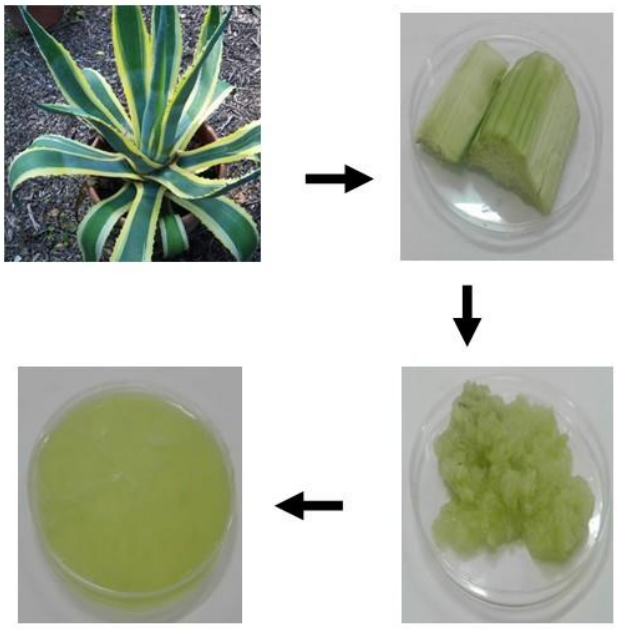

Fig.2. GAA.

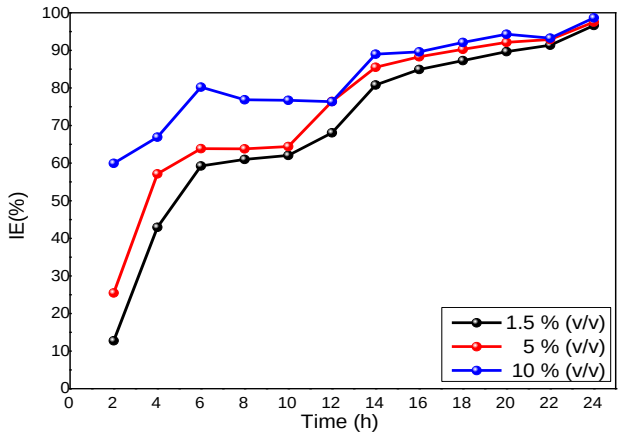

Fig.3. Variation in the GAA inhibitory efficacy at different concentrations on AISI 410 in 0.5M H_2SO_4, according to time

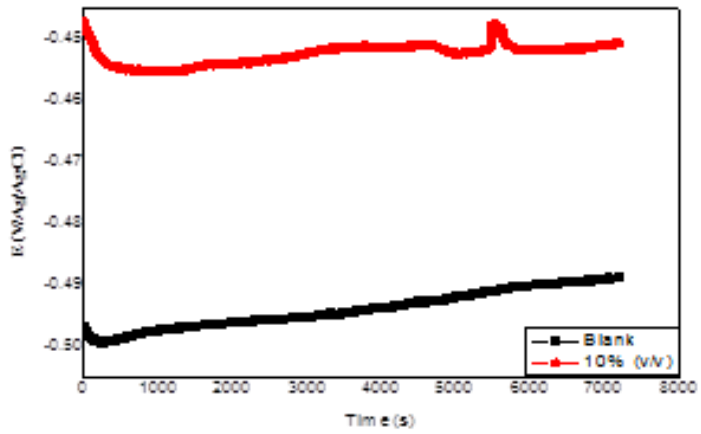

Fig.4. Open circuit potential of AISI 410 according to time in 0.5M H_2SO_4 either with or without 10% (v/v) GAA, after 2 hours immersion at 25°C

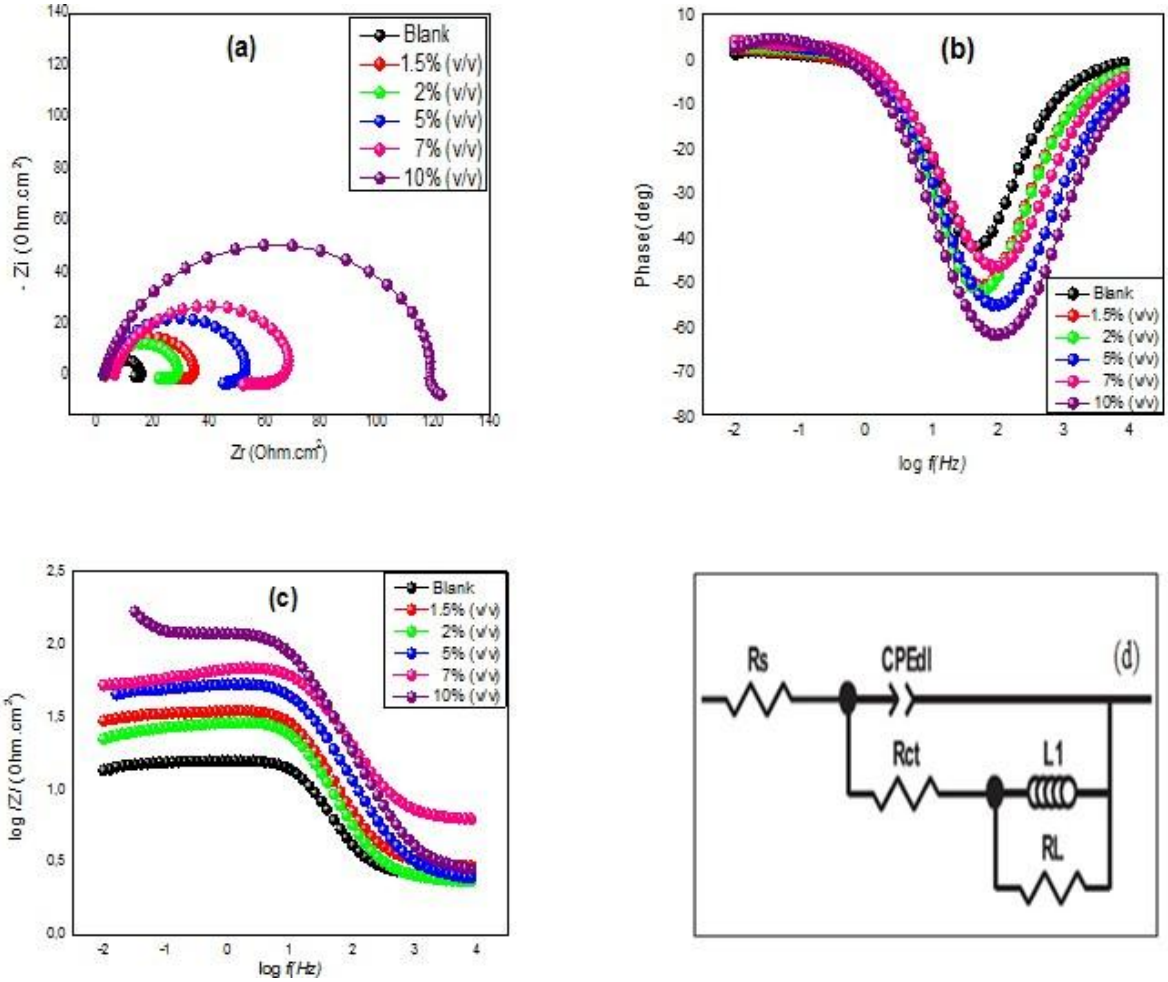

Fig. 5. Electrochemical impedance diagrams for AISI 410 in 0.5M H_2SO_4 either with or without GAA at various concentrations after 2 h immersion at 25°C: (a) Nyquist; (b) Bode according to phase angle; (c) Bode according to the module and (d) Equivalent electrical circuit

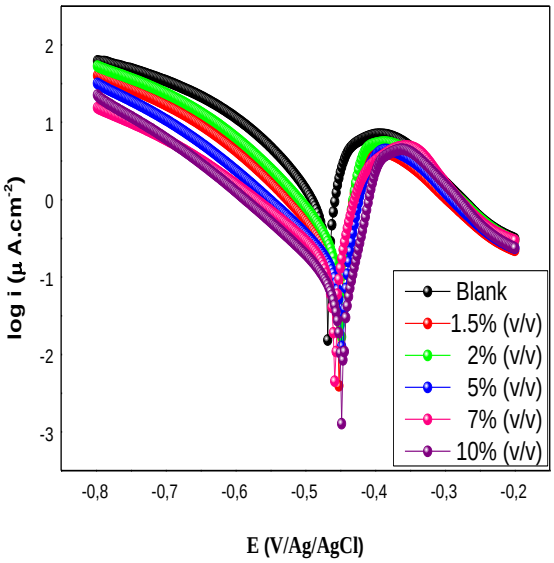

Fig.6. Potentiodynamic polarization curves of AISI 410 in 0.5M H_2SO_4, either with or without GAA at different concentrations, after 2 h immersion, at 25°C

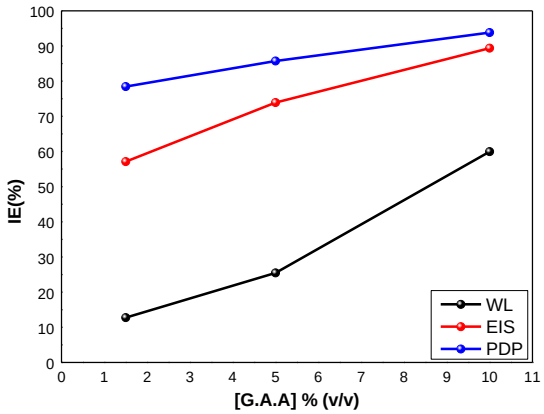

Fig.7. Influence of GAA concentration on the inhibitor efficacy by different methods: (a) WL (b) EIS and (c) PDP

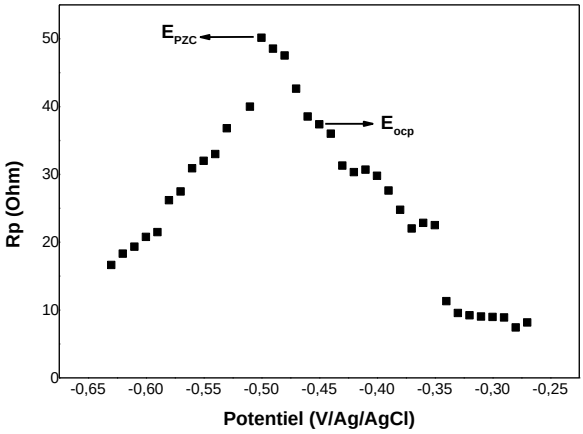

Fig.8. Variation of the polarization resistance according to the AISI 410 potential in 0.5M H_2SO_4 with 10% (v/v) GAA

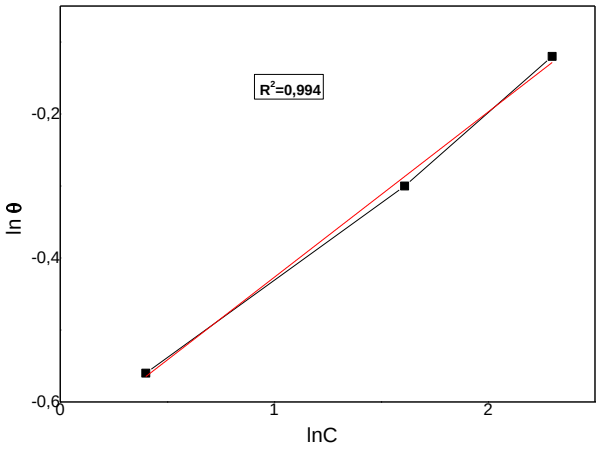

Fig.9. Freundlich adsorption isotherm of AISI 410 in 0.5M H_2SO_4 with GAA, after 2h immersion

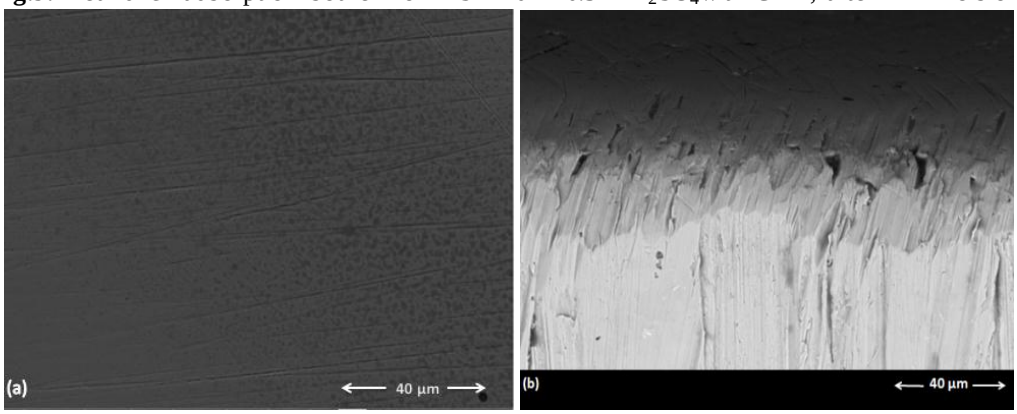

Fig.10. Micrographs (SEM) of AISI 410 surface: (a) Front view and (b) Cross section

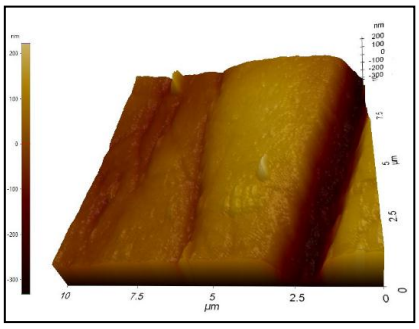

Fig. 11. Micrograph (AFM) of AISI 410

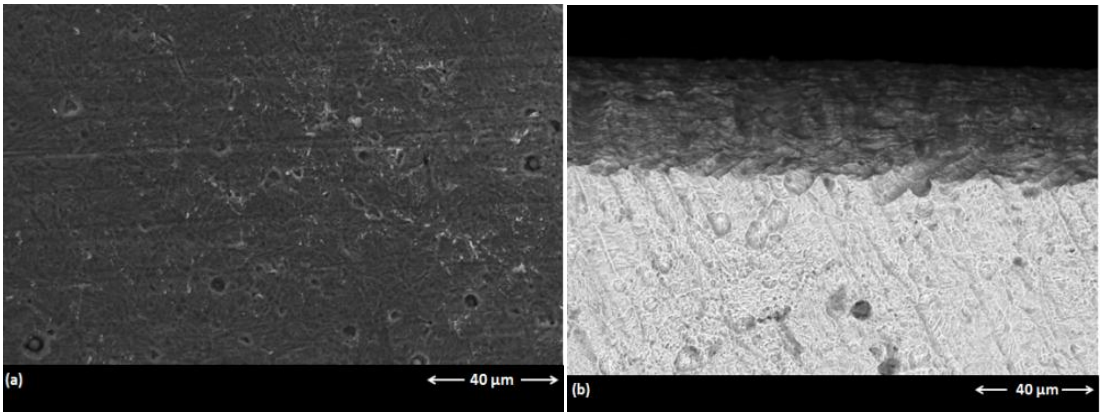

Fig.12. Micrographs (SEM) of AISI 410 surface in 0.5M H_2SO_4 after 2h immersion at 25°C: (a) Front view, and (b) Cross section

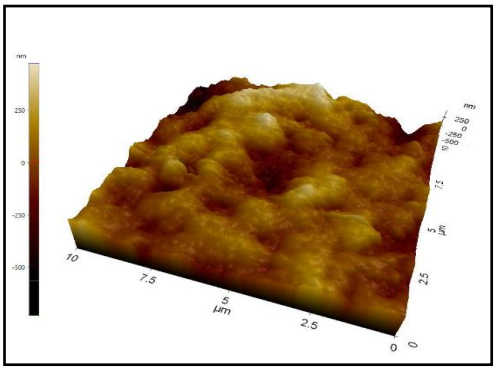

Fig.13. Micrograph (AFM) of AISI410 in 0.5M H_2SO_4, after 2 h immersion at 25°C

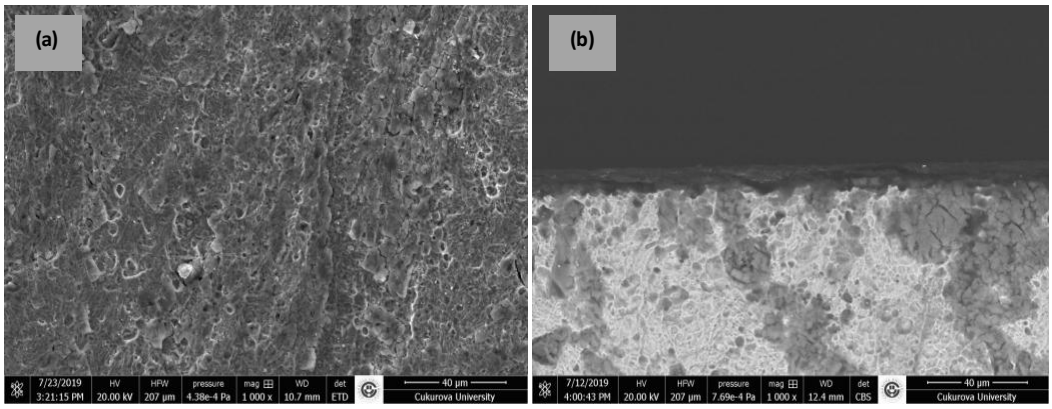

Fig.14. Micrographs (SEM) of AISI 410 in 0.5M H_2SO_4in the presence of 10% (v/v) GAA, after 2h immersion at 25°C: (a) Front view and (b) Cross section

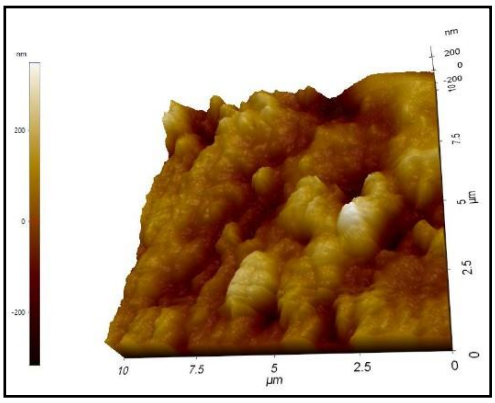

Fig.15. Micrograph (AFM) of AISI 410 in 0.5M $H_2SO_4$with 10% (v/v) GAA after 2h immersion at 25°C

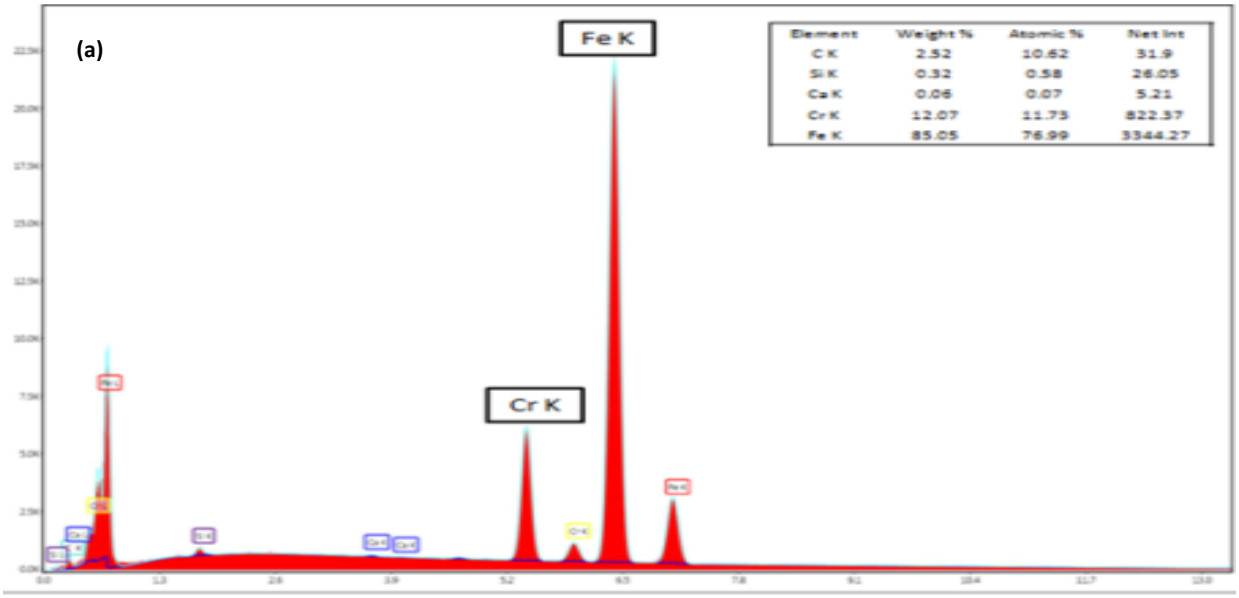

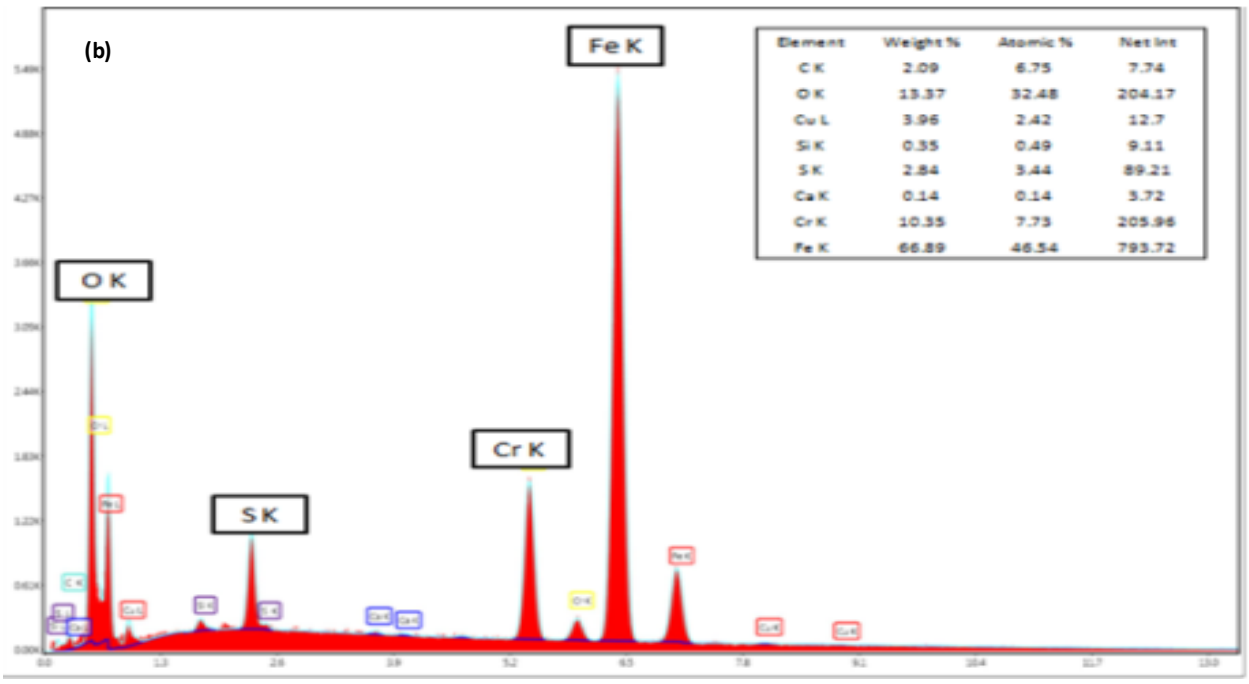

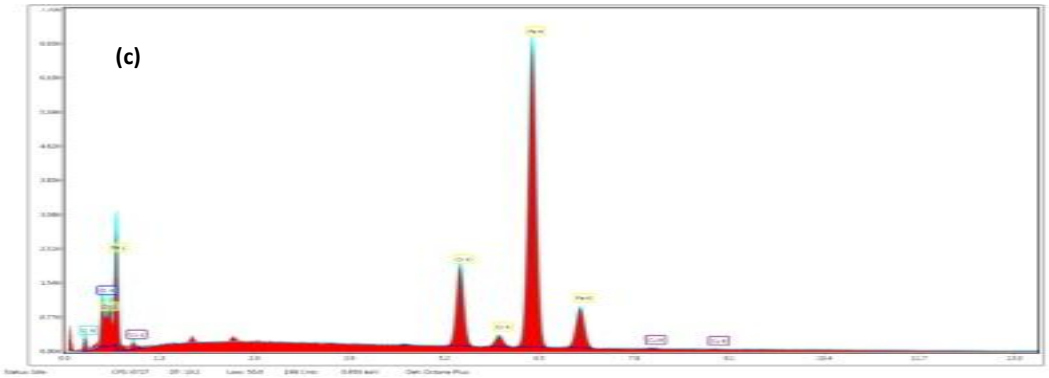

Fig.16. EDX spectrum (a) of AISI 410, (b) in 0.5M H_2SO_4 and (c) with 10% (v/v) GAA, after 2h immersion at 25°C

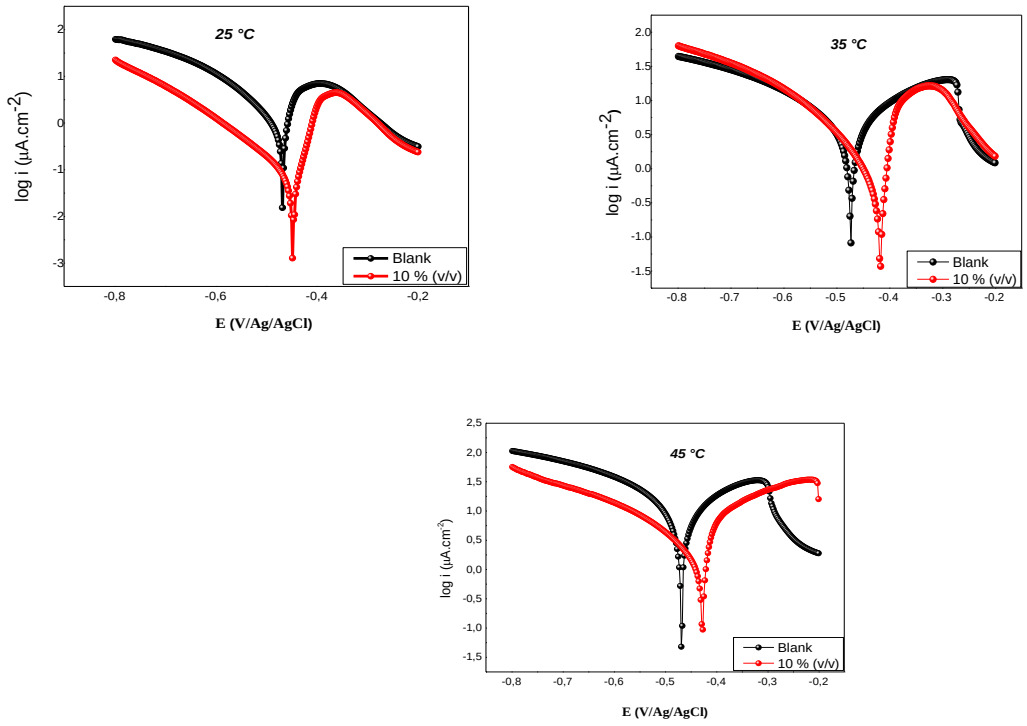

Fig .17. Temperature effect on AISI 410 polarization in 0.5M H_2SO_4 either with or without 10% (v/v) GAA, after 2h immersion

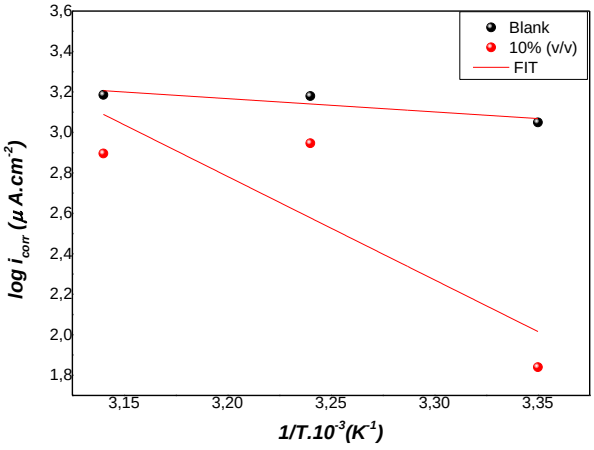

Fig.18. Arrhenius straight lines of log i_{corr} according to 1/T of AISI 410 in 0.5M H_2SO_4 either with or without 10% (v/v) GAA

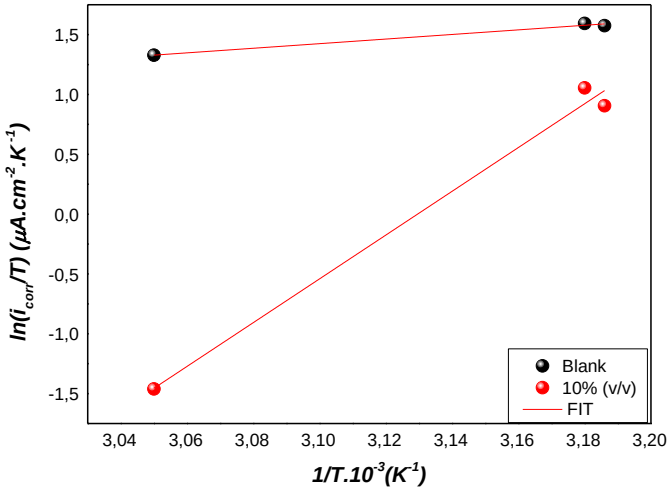

Fig.19. Arrhenius straight lines of ln (i_{corr}/T) according to 1/T of AISI 410 in 0.5M H_2SO_4 either with or without 10% (v/v) GAA

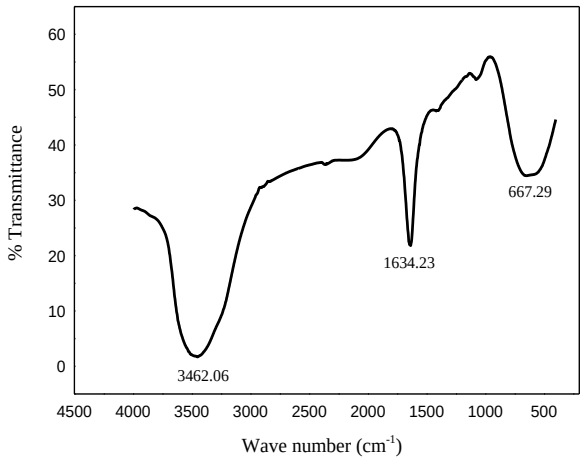

Fig.20. FT-IR spectrum of GAA

4. Conclusions

The object of this work is to study the Grated *Agave Americana* effect as an ecological corrosion inhibitor of AISI 410 in 0.5M H_2SO_4. The results obtained are as follows:

- ✓ Presence of a capacitive loop followed by a second inductive
- ✓ The adsorption of GAA obeys to Freundlich isotherm
- ✓ GAA behaves as a mixed inhibitor
- ✓ The surface of the AISI410 is positively charged
- ✓ The molecules of GAA are physisorbed
- ✓ The thermodynamic parameters of adsorption indicate that the GAA adsorption process on AISI 410 surface is spontaneous and favorable, and it occurs by a physical adsorption mechanism
- ✓ The best inhibitory efficacy of GAA was obtained at 25°C
- ✓ The FT-IR analysis of the GAA confirms the presence of functional groupings that are responsible for the inhibition
- ✓ The SEM-EDX and AFM micrographs confirm the results obtained by the gravimetric method and the electrochemical, stationary (potentiodynamic) and transient (EIS) methods

Acknowledgements

The authors are greatly thankful to Pr.Gülfeza Kardaş from the Çukurova University (Adana, Turkey), and also to Mrs. Nora Zennadi for her help with translation work.

References

[1] J. Yan, M.Gao and X. Zeng. (2010). Study on microstructure and mechanical properties of 304 stainless steel joints by TIG, laser, and laser-TIG hybrid welding. Optics and Lasers in Engineering. 48: 512–517.

[2] A. Ehsani, M.G. Mahjani, M. Hosseini, R. Safari, R. Moshrefi and H.M. Shiri. (2017). Evaluation of *Thymus vulgaris* plant extract as an eco-friendly corrosion inhibitor for stainless steel 304 in acidic solution by means of electrochemical impedance spectroscopy, electrochemical noise analysis and density functional theory. Journal of colloid and interface science. 490: 444-451.

[3] N.J. Laycock and R.C. Newman. (1997). Localized dissolution kinetics, salt films, and pitting potentials. Corrosion Science. 39(10–11): 71–90.

[4] H.P. Leckie and H.H. Uhlig. (1966). Environmental factors affecting the critical potential for pitting in 18-8 stainless steel. Journal of The Electrochemical Society. 113 (12): 1262-1268.

[5] R.W. Revie. (2000). Uhlig's. Corrosion Handbook, second ed. John Wiley & Sons, NY. 676.

[6] C.X. Li and T. Bell. (2006). Corrosion properties of plasma nitrided AISI 410 martensitic stainless steel in 3.5% NaCl and 1% HCl aqueous solutions. Corrosion Science. 48 (8): 2036-2049.

[7] P.D. Krell, S. Li and H. Cong. (2017). Synergistic effect of temperature and HCl concentration on the degradation of AISI 410 stainless steel. Corrosion Science. 122: 41-52.

[8] A. Rustandi, G. Sirait, A. Saputra, and Y. Sadeli. (2018). The use of electrochemical impedance spectroscopy method for corrosion resistance evaluation of 2205 and 410s stainless steels in aqueous sodium chloride solution. In IOP Conference Series: Materials Science and Engineering. 299 (1): 012053.

[9] A.S. Fouda, K. Shalabi and N.H. Mohamed. (2014). International Journal of Innovative Research in Science, Engineering and Technology. 3: 9861–9875.

[10] A.S. Fouda, F.M. El-Taweel, and M. Elgamil. (2017). Corrosion inhibition of aluminum in hydrochloric acid solution using some pyrazolocarbothioamide derivatives. International Journal of Electrochemical Science. 12(12): 11397-11418.

[11]D. Daoud, T. Douadi, S. Issaadi and S. Chafaa. (2014). Adsorption and corrosion inhibition of new synthesized thiophene Schiff base on mild steel X52 in HCl and H_2SO_4 solutions. Corrosion science. 79: 50-58.

[12] X. He, Y. Jiang, C. Li, W. Wang, B. Hou and L. Wu. (2014). Inhibition properties and adsorption behaviour of imidazole and 2-phenyl-2-imidazoline on AA5052 in 1.0M HCl solution. Corrosion Science. 83: 124-136.

[13] K.S. Beenakumari. (2011). Inhibitory effects of *Murraya koenigii* (curry leaf) leaf extract on the corrosion of mild steel in 1 M HCl. Green Chemistry Letters and Reviews. 4(2): 117-120.

[14] P.B. Raja and M.G. Sethuraman. (2008). Natural products as corrosion inhibitor for metals in corrosive media—a review. Materials Letters. 62(1): 113-116.

[15] M.A. Dar. (2011). A review: plant extracts and oils as corrosion inhibitors in aggressive media. Industrial Lubrication and Tribology. 63. 227–233.

[16] H. Ashassi-Sorkhabi, D. Seifzadeh, and M.G. Hosseini. (2008). EN, EIS and polarization studies to evaluate the inhibition effect of 3H-phenothiazin-3-one, 7-dimethylamin on mild steel corrosion in 1M HCl solution. Corrosion Science. 50(12): 3363-3370.

[17] O. Sanni, A.P. Popoola and O.S. Fayomi. (2020). Adsorption and performance evaluation of green corrosion inhibitor from industrial waste on uns n08904 stainless steel subjected to chloride solution. Journal of Chemical Technology & Metallurgy. 55(2): 449-458.

[18] W.M.K.W.M. Ikhmal, M.Y.N. Yasmin, M.F.F. Maria, S.M. Syaizwadi, W.A.W. Rafizah, M.G.M. Sabri and B.M. Zahid. (2020). Evaluating the performance of *Andrographis paniculata* leaves extract as additive for corrosion protection of stainless steel 316L in seawater. International Journal of Corrosion and Scale Inhibition. 9(1): 118-133.

[19] A.M.B. Hamissa, M. Seffen, B. Aliakbarian, A.A. Casazza, P. Perego and A. Converti. (2012). Phenolics extraction from *Agave americana* (L.) leaves using high-temperature, high-pressure reactor. Food and bioproducts processing. 90(1): 17-21.

[20] S. Athmani, S. Abderrahmane, F. Benachour and G. Kardas. (2018). A study of the effect of *Agave Americana* extract inhibitor on the corrosion of mild steel in 0.5 M H_2SO_4. Materials Research Express.

[21] A. Oulabbas and S. Abderrahmane. (2018). Natural extract of *Opuntia ficus indica* as green inhibitor for corrosion of XC52 steel in 1M H_3PO_4. Materials Research Express.

[22] F. Krid, E. Zouaoui and M.S. Medjram. (2018). Aqueous extracts of *Opuntia Ficus-Indica* as green corrosion inhibitor of A283C carbon steel in 1N sulfuric acid solution. Chemistry & Chemical Technology. 12: 405-409.

[23] J.P. Flores de los Ríos, M. Sánchez-Carrillo, C.G. Nava-Dino, J.G. Chacón-Nava, J.G. González-

Rodríguez, E.Huape-Padilla, M.A. Neri-Flores and A. Martínez-Villafañe. (2015). *Opuntia ficus-indica* extract as green corrosion inhibitor for carbon steel in 1 M HCl solution. Journal of Spectroscopy. ID 714692.

[24] M. Amensour, E. Sendra, J.A. Pérez-Alvarez, N. Skali-Senhaji, J. Abrini and J. Fernández-López. (2010). Antioxidant activity and chemical content of methanol and ethanol extracts from leaves of rockrose (*Cistus ladaniferus*). Plant foods for human nutrition. 65: 170-178.

[25] R. Bajwa, I. Mukhtar and S. Mushtaq. (2010). New report of *Alternaria alternata* causing leaf spot of Aloe vera in Pakistan. Canadian Journal of Plant Pathology. 32. 490-492.

[26] M. Mehdipour, B. Ramezanzadeh and S.Y. Arman. (2015). Electrochemical noise investigation of Aloe plant extract as green inhibitor on the corrosion of stainless steel in 1M H_2SO_4. Journal of Industrial and Engineering Chemistry. 21. 318-327.

[27] A. Ostovari, S.M. Hoseinieh, M. Peikari, S.R. Shadizadeh and S.J. Hashemi. (2009).Corrosion inhibition of mild steel in 1 M HCl solution by henna extract: A comparative study of the inhibition by henna and its constituents (Lawsone, Gallic acid, α-d-Glucose and Tannic acid).Corrosion Science. 51. 1935-1949.

[28] M. Lebrini, F. Robert, A. Lecante and C. Roos, C. (2011). Corrosion inhibition of C38 steel in 1M hydrochloric acid medium by alkaloids extract from *Oxandra asbeckii* plant. Corrosion Science. 53. 687-695.

[29] G. Ji, S. Anjum, S. Sundaram and R. Prakash. (2015). Musa paradisica peel extract as green corrosion inhibitor for mild steel in HCl solution. Corrosion Science. 90.107-117.

[30] A. Shakeel, Saifullah, A. Mudasir, L.S. Babu and I. Saiqa. (2016). Green synthesis of silver nanoparticles using *Azadirachta indica* aqueous leaf extract. Journal of Radiation Research and Applied Sciences. 9. 1-7.

[31] A. Khadraoui, A. Khelifa, H. Boutoumi and B. Hammouti. (2014). *Mentha pulegium* extract as a natural product for the inhibition of corrosion. Part I: electrochemical studies. Natural product research. 28. 1206-1209.

[32] A.M. Abdel-Gaber, B.A. Abd-El Nabey, I.M. Sidahmed, A.M. El-Zayady and M. Saadawy. (2006). Effect of temperature on inhibitive action of damsissa extract on the corrosion of steel in acidic media. Corrosion. 62. 293-299.

[33] F. Ekanem, S.A. Umoren, I.I. Udousoro and A.P. Udoh. (2010). Inhibition of mild steel corrosion in HCl using pineapple leaves (*Ananas comosus* L.) extract. Journal of materials science. 45. 5558-5566.

[34] O. Eddy, S.A. Odoemelam and A.O. Odiongenyi. (2009). Joint effect of halides and ethanol extract of *Lasianthera africana* on inhibition of corrosion of mild steel in H_2SO_4. Journal of applied electrochemistry. 39: 849-857.

[35] P.C. Okafor and E.E. Ebenso. (2007). Inhibitive action of *Carica papaya* extracts on the corrosion of mild steel in acidic media and their adsorption characteristics. Pigment & Resin Technology. 36. 134-140.

[36] A.K. Satapathy, G. Gunasekaran, S.C. Sahoo, K. Amit and R.V. Rodrigues. (2009).Corrosion inhibition by *Justicia gendarussa* plant extract in hydrochloric acid solution. Corrosion science. 51: 2848-2856.

[37] J.C. Rocha, J.A.C.P. Gomes and E.D. Elia. (2010). Corrosion inhibition of carbon steel in hydrochloric acid solution by fruit peel aqueous extracts. Corrosion Science. *52*. 2341-2348.

[38] M. Behpour, S.M. Ghoreishi, M. Khayat Kashani and N. Soltani. (2011). The effect of two oleo-gum resin exudate from *Ferula assa-foetida* and *Dorema ammoniacum* on mild steel corrosion in acidic media. Corrosion Science. 53: 2489-2501.

[39] M. Shabani-Nooshabadi, F.S. Hoseiny and Y. Jafari. (2014). Corrosion inhibition of copper by *Ephedra sarcocarpa* plant extract as green corrosion inhibitor in strong acidic medium. Analytical and Bioanalytical Electrochemistry. 6: 341-354.

[40] M. Shabani-Nooshabadi, F.S. Hoseiny and Y. Jafari. (2015). Green approach to corrosion inhibition of copper by the extract of *Calligonum comosum* in strong acidic medium. Metallurgical and Materials Transactions A. 46: 293-299.

[41] Y. Lekbach, Z. Li, D. Xu, S. El Abed, Y. Dong, D. Liu, T. Gu, S.I. Koraichi, K. Yang and F. Wang. (2019). *Salvia officinalis* extract mitigates the microbiologically influenced corrosion of 304L stainless steel by *Pseudomonas aeruginosa* biofilm. Bioelectrochemistry. 128.193-203.

[42] R. Haldhar, D. Prasad and A. Saxena. (2018). *Armoracia rusticana* as sustainable and eco-friendly corrosion inhibitor for mild steel in 0.5M sulphuric acid: Experimental and theoretical investigations. Journal of Environmental Chemical Engineering. 6. 5230-5238.

[43] R. Haldhar, D. Prasad and A. Saxena. (2018). *Myristica fragrans* extract as an eco-friendly corrosion inhibitor for mild steel in 0.5M H_2SO_4 solution. Journal of Environmental Chemical Engineering. 6: 2290-2301.

[44] A. Saxena, D. Prasad and R. Haldhar. (2018). Investigation of corrosion inhibition effect and adsorption activities of *Cuscuta reflexa* extract for

mild steel in 0.5 M H_2SO_4. Bioelectrochemistry. 124: 156-164.

[45] A. Saxena, D. Prasad, R. Haldhar, G. Singh and A. Kumar. (2018). Use of *Sida cordifolia* extract as green corrosion inhibitor for mild steel in 0.5M H_2SO_4. Journal of Environmental Chemical Engineering. 6. 694-700.

[46] A. Sedik, D. Lerari, A. Salci, S. Athmani, K. Bachari, İ.H. Gecibesler and R. Solmaz. (2020). Dardagan fruit extract as eco-friendly corrosion inhibitor for mild steel in 1 M HCl: Electrochemical and surface morphological studies. Journal of the Taiwan Institute of Chemical Engineers. 107: 189-200.

[47] P.R. SIVAKUMAR and A.P. SRIKANTH. (2020). Green corrosion inhibitor: A comparative study. Indian Academy of Sciences. 45(1): 1-11.

[48] D.P. Supriya Bangeraand Vijaya. (2020). Alva Aqueous Extract of *Macaranga Peltata* Leaves—Green Corrosion Inhibitor for Mild Steel in Hydrochloric Acid Medium. Surface Engineering and Applied Electrochemistry. 56(2): 259–266.

[49] D.Q. Zhang, Q.R. Cai, X.M. He, L.X. Gao and G.S. Kim. (2009). Corrosion inhibition and adsorption behaviour of methionine on copper in HCl and synergistic effect of zinc ions. Materials Chemistry and Physics. 114: 612–617.

[50] E. McCafferty. (2005). Validation of corrosion rates measured by the tafel extrapolation method. Corrosion Science. 47: 3202-3215.

[51] M.K. Pavithra, T.V. Venkatesha, M.K.P. Kumar and H.C. Tondan. (2012). Inhibition of mild steel corrosion by Rabeprazole sulphide. Corrosion Science. 60: 104-111.

[52] N. Raghavendra, L.V. Hublikar, S.M. Patil, P.J. Ganiger and A.S. Bhinge. (2019). Efficiency of sapota leaf extract against aluminium corrosion in a 3M sodium hydroxide hostile fluid atmosphere: a green and sustainable approach. Bulletin of Materials Science. 42: 226.

[53] R. Idouhli, A. Abouelfda, A. Benyaich and A. Aityoub. (2016). *Cuminum Cyminum* Extract-A Green Corrosion Inhibitor of S300 Steel in 1M HCl. Chemical and Process Engineering. 44: 16–25.

[54] D. Jeroundi, H. Elmsellem, S. Chakroune. (2016). Physicochemical study and corrosion inhibition potential of dithiolo[4,5-b][1,4]dithiepine for mild steel in acidic medium. Journal of Materials and Environmental Science. 7: 4024–4035.

[55] J. Haque, K.R. Ansari, V. Srivastava, M.A. Quraishi and I.B. Obot. (2017). Pyrimidine derivatives as novel acidizing corrosion inhibitors for N80 steel useful for petroleum industry: A combined experimental and theoretical approach. Journal of Industrial and Engineering Chemistry. 49: 176–188.

[56] A. Singh, K. Ansari, M. Quraishi and H. Lgaz. (2019). Effect of electron donating functional groups on corrosion inhibition of J55 steel in a sweet corrosive environment: experimental, density functional theory, and molecular dynamic simulation. Materials (Basel). 12: 17.

[57] Z. Ghazi, H. ELmssellem, M. Ramdani, A. Chetouani, R. Rmil, A. Aouniti and B. Hammouti. (2014). Corrosion inhibition by naturally occurring substance containing *Opuntia-Ficus Indica* extract on the corrosion of steel in hydrochloric acid. Journal of Chemical and Pharmaceutical Research. 6: 14171425.

[58] A. Popova, E. Sokolova, S. Raicheva and M. Christov. (2003). AC and DC study of the temperature effect on mild steel corrosion in acid media in the presence of benzimidazole derivatives. Corrosion Science. 45. 33–58.

[59] T. Szauer and A. Brandt. (1981). Adsorption of oleates of various amines on iron in acidic solution, Electrochemistry Acta. 26. 1253–1256.

[60] A. Popova. (2007). Temperature effect on mild steel corrosion in acid media in presence of azoles. Corrosion Science. 49(5): 2144-2158.

[61] A.S. Fouda, K. Shalabi and M.S. Shaaban. (2019). Synergistic Effect of Potassium Iodide on Corrosion Inhibition of Carbon Steel by *Achillea santolina* Extract in Hydrochloric Acid Solution. Journal of Bio-and Tribo-Corrosion. 5(3): 71.

[62] P. Muthukrishnan, B. Jeyaprabha and P. Prakash. (2013). Corrosion inhibition and adsorption behavior of *Setaria verticillata* leaf extract in 1M sulphuric acid. Journal of materials engineering and performance. 22(12): 3792-3800.

[63] V.S. Sastri, E. Ghali and M. Elboujdaini. (2007). Corrosion Prevention and Protection: Practical Solutions, Wiley, New Jersey.

[64] H. Hassannejad and A. Nouri. (2018). Sunflower seed hull extract as a novel green corrosion inhibitor for mild steel in HCl solution. Journal of Molecular Liquids. 254. 377-382.

[65] S.A. Umoren, U.M. Eduok. (2016). Application of carbohydrate polymers as corrosion inhibitors for metal substrates in different media: a review. Carbohydrate polymers. 140: 314-341.

[66] N.I.N. Haris, S. Sobri, Y.A. Yusof and N. Kassim. (2019). Oil palm empty fruit bunch extract and powder as an eco-friendly corrosion inhibitor for mild steel: A comparison study. Materials and Corrosion. 70(12): 2326-2333.